The S_3^- Ion Is Stable in Geological Fluids at Elevated Temperatures and Pressures

Gleb S. Pokrovski, *et al.*

Science **331**, 1052 (2011);
DOI: 10.1126/science.1199911

21. K. Meyer, E. Bill, B. Mienert, T. Weyhermueller, K. Wieghardt, *J. Am. Chem. Soc.* **121**, 4859 (1999).
22. F. Tiago de Oliveira *et al.*, *Science* **315**, 835 (2007).
23. The $S = 3/2$ state was found to be higher in energy by 0.735 eV (16.9 kcal/mol) at the B3LYP level.
24. For a perfectly C_3-symmetric molecule, the angle would be 180°.
25. The indophenol method is particularly sensitive to nitrogen determination from ammonia: NH_3 is oxidized in an alkaline hypochlorite solution to NH_2Cl, which, in the presence of sodium nitroprusside as a catalyst, subsequently reacts with a phenol (thymol) to yield the deep blue, spectrophotometrically quantified indophenol.
26. M. Berthelot, *Rep. Chim. Appl.* **1**, 284 (1859).
27. We acknowledge funding from Friedrich-Alexander-University Erlangen-Nuremberg and the Deutsche Forschungsgemeinschaft (K.M.); Fonds der Chemischen Industrie (M.M.K.); and the Department of Energy Office of Basic Energy Sciences (DE-FG02-08ER15996) and the Camille and Henry Dreyfus Foundation (J.M.S.). J. Sutter is gratefully acknowledged for collecting the spectroscopic data, and K. Wieghardt and E. Bill (Max-Planck-Institut for Bioinorganic Chemistry, Mülheim/Ruhr, Germany) for helpful discussions. The crystallographic data CCDC-786059 (**2** at 35 K) and CCDC-786060 (**2** at 100 K) can be obtained free at www.ccdc.cam.ac.uk/data_request/cif (or from Cambridge Crystallographic Data Centre, 12 Union Road, Cambridge, CB2 1EZ, UK; fax: ++44-1223-336-033; e-mail: deposit@ccdc.cam.ac.uk).

Supporting Online Material

www.sciencemag.org/cgi/content/full/331/6020/1049/DC1
Materials and Methods
Figs. S1 to S11
Tables S1 to S6
References

27 September 2010; accepted 25 January 2011
10.1126/science.1198315

The S_3^- Ion Is Stable in Geological Fluids at Elevated Temperatures and Pressures

Gleb S. Pokrovski[1]* and Leonid S. Dubrovinsky[2]

The chemical speciation of sulfur in geological fluids is a controlling factor in a number of processes on Earth. The two major chemical forms of sulfur in crustal fluids over a wide range of temperature and pressure are believed to be sulfate and sulfide; however, we use in situ Raman spectroscopy to show that the dominant stable form of sulfur in aqueous solution above 250°C and 0.5 gigapascal is the trisulfur ion S_3^-. The large stability range of S_3^- enables efficient transport and concentration of sulfur and gold by geological fluids in deep metamorphic and subduction-zone settings. Furthermore, the formation of S_3^- requires a revision of sulfur isotope–fractionation models between sulfides and sulfates in natural fluids.

Sulfur participates in numerous inorganic and biological reactions over a wide range of temperatures and pressures (*1*–*3*), during which it often exhibits large fractionations among its stable isotopes (*4*–*7*) and transforms between its multiple valence states and chemical forms. Earth's surface and shallow crust are characterized by a large variation in sulfur forms, with sulfide (S^{2-}: $H_2S/HS^-/S^{2-}$) and sulfate (S^{6+}: HSO_4^-/SO_4^{2-}) being the most common. Other sulfur species (for instance, elemental sulfur, sulfite, thiosulfate, polysulfides, polythionates, and organic sulfur) form as reaction intermediates in the sulfate-sulfide redox cycle but are relatively minor or thermodynamically metastable at near-surface conditions (*1*, *2*). The sulfur speciation in deep and hot fluids from hydrothermal-magmatic systems and subduction zones hosting the major part of metallic resources on Earth (*3*) is far less constrained. This is due to intrinsic difficulties in studying such fluid systems, which are strongly sensitive to temperature, pressure, and redox conditions. For example, sulfur solubility in water increases by about five orders of magnitude over the hydrothermal temperature range (20° to 500°C) (*8*, *9*). Intermediate-valence species, such as SO_2, that are potentially important in shallow magmatic-hydrothermal systems (*3*) tend to disproportionate rapidly into sulfate and hydrogen sulfide (with or without native sulfur) in the aqueous fluid or vapor phase on cooling (*8*–*11*). The rates of chemical and isotopic equilibration between sulfates and sulfides in an acidic aqueous solution at supercritical temper-

[1]Géosciences Environnement Toulouse (GET, ex-LMTG), UMR 5563 of CNRS, Université Paul Sabatier, 14, avenue Edouard Belin, F-31400 Toulouse, France. [2]Bayerisches Geoinstitut, Universität Bayreuth, D-95440 Bayreuth, Germany.
*To whom correspondence should be addressed. E-mail: gleb.pokrovski@get.obs-mip.fr

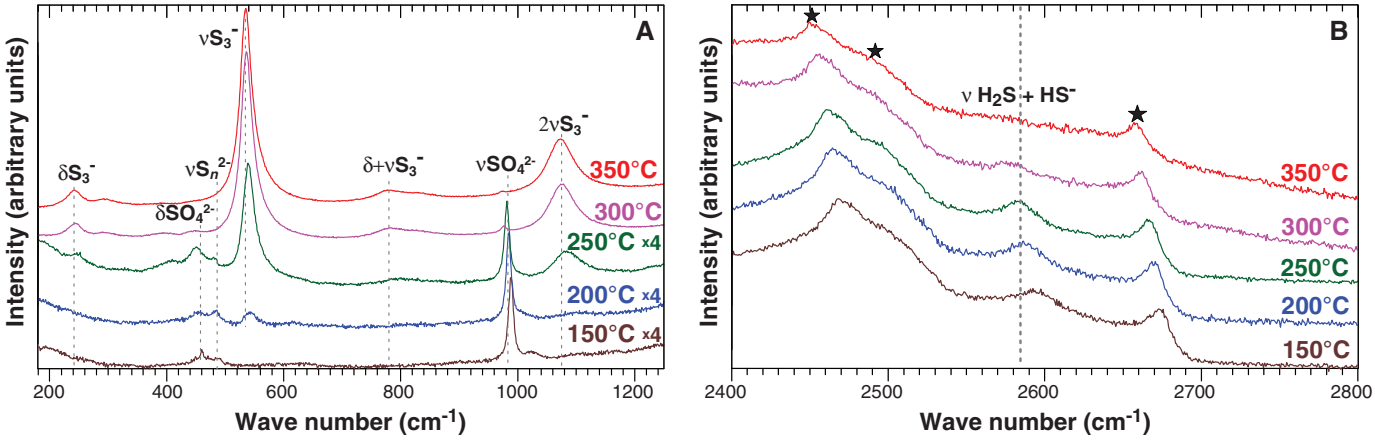

Fig. 1. (**A**) Raman spectra of an aqueous solution of 1 mol/kg potassium thiosulfate ($K_2S_2O_3$) at equilibrium at temperatures ranging from 150° to 350°C and pressures of 1.5 ± 0.3 GPa at the S-S and S-O bond-vibration region below 1250 cm^{-1}. Spectra at 150° to 250°C are magnified by a factor of 4 to emphasize small bands. (**B**) Raman spectra showing the S-H bands of H_2S and HS^-. Spectra are normalized to 30-s acquisition time and offset vertically for clarity. Vertical dashed lines denote the vibration modes (ν = stretching, δ = bending) and positions of major Raman peaks for the indicated species; stars show the bands of diamond. The frequency shifts of the bands with temperature are typical for aqueous species. Spectra demonstrate the reversible formation of the S_3^- ion at 300° and 350°C at the expense of sulfate and sulfide, which are stable at lower temperatures (*13*).

atures are too fast (*4*) to allow a magmatic-hydrothermal fluid to preserve its original sulfur speciation on cooling. Thus, most aqueous fluids quenched or trapped as inclusions in minerals, both in nature and in the laboratory, contain almost exclusively sulfate and sulfide (*2*, *11*, *12*) and may not reflect the true speciation at high temperature and pressure.

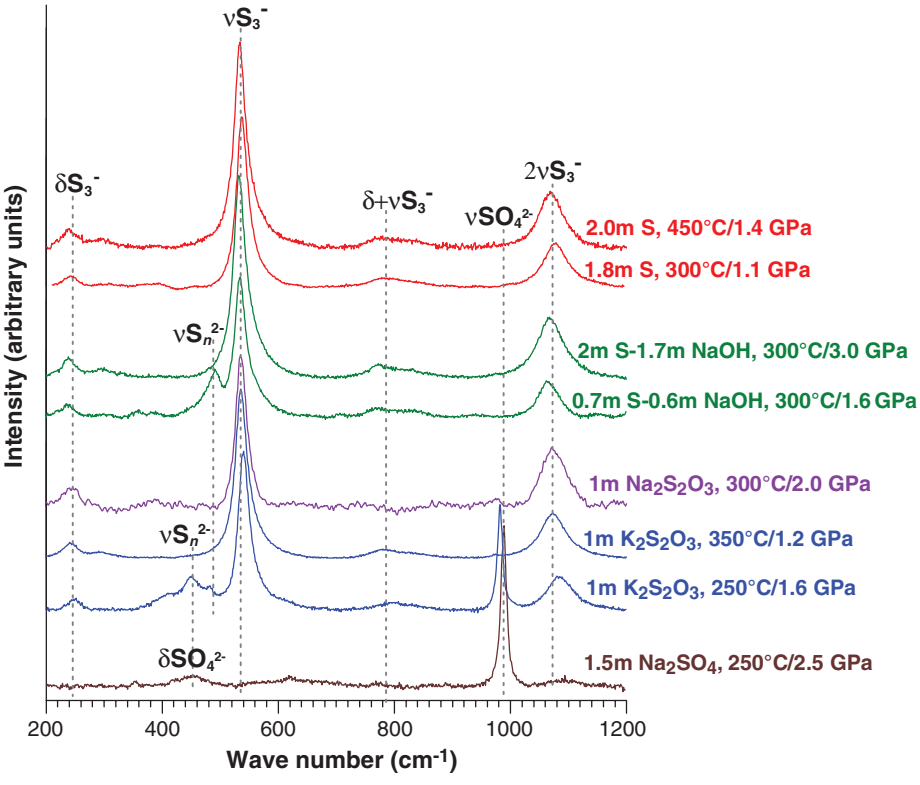

Fig. 2. Selected Raman spectra of sulfur-bearing aqueous fluids at steady-state conditions, showing the systematic formation of S_3^-. Spectra were baseline subtracted and scaled for better comparison between the different experiments. Vertical dashed lines denote the S-S and S-O vibration modes and positions of the main Raman bands of S_3^-, sulfate, and polysulfide (when present). Solute concentrations are expressed in moles per kilogram of fluid (m).

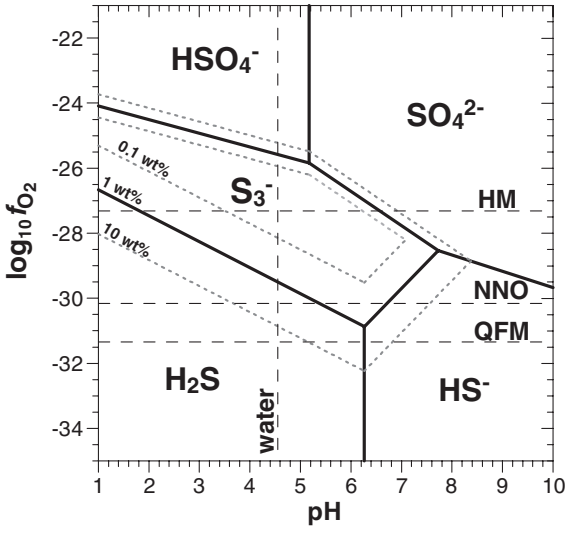

Fig. 3. Stability domains of the trisulfur ion S_3^-, sulfate, and sulfide in an aqueous solution of total dissolved sulfur concentration of 1 wt %, as a function of oxygen fugacity ($\log_{10}f_{O2}$, in bars) and acidity (pH = $-\log_{10}m_{H+}$, in moles per kilogram) at 350°C and 0.5 GPa. The diagram was constructed using the stability constants of S_3^- derived in this study (*13*, *22*) and those of sulfate and sulfide from (*8*). Bold lines delimit the fields of predominance of each aqueous sulfur form. Horizontal dashed lines indicate the oxygen fugacity of the major mineral buffers (HM, hematite-magnetite; NNO, nickel-nickel oxide; QFM, quartz-fayalite-magnetite); the vertical dashed line stands for the neutrality point of pure water. Variations in total sulfur concentration by ±one order of magnitude (from 0.1 to 10 wt %, shown by dotted lines) result in changes in the stability domain of S_3^- by ±1.5 and ±0.5 $\log_{10}f_{O2}$ units for the sulfide and sulfate side, respectively.

Because of these limitations, the thermodynamic and kinetic properties and isotope fractionation could be investigated in detail only for the two aqueous end members, sulfate and sulfide, at temperature and pressure conditions of shallow magmatic-hydrothermal systems (*2*–*4*, *8*). Together with chloride, these forms are regarded as the major transporting agents of metals in hydrothermal and metamorphic ore-bearing fluids (*2*, *3*, *11*, *12*) and as responsible for sulfur isotope records in sulfide and sulfate minerals formed (*2*, *4*). However, this simplicity of sulfur aqueous chemistry may only be apparent because of the lack of in situ approaches for analyzing geological fluids at elevated temperatures and pressures.

To fill this gap, we employed in situ Raman spectroscopy in a diamond anvil cell at 25° to 450°C and 0.5 to 3.5 GPa to measure the identity and stability of S-bearing species in model aqueous solutions of thiosulfate and sulfur across a range of acidity ($1 < pH < 7$) and of sulfur concentration [0.6 to 6 weight percent (wt %)] that are representative of crustal and subduction-zone fluids. These experimental conditions provide acidity and redox control on the system through the sulfate-sulfide equilibrium and can fix oxygen fugacity close to the magnetite-hematite mineral buffer. They also allow for the identification of the dominant S species directly from their characteristic Raman spectra (*13*).

Our data indicate the preponderance of sulfate and sulfide in solution at < 250°C and 0.5 to 3.5 GPa (Fig. 1), in agreement with thermodynamic predictions (fig. S1) (*2*, *4*, *8*, *12*). In contrast, at higher temperatures, we systematically found that the dominant form of sulfur was the trisulfur S_3^- radical ion (Figs. 1 and 2). This ion is characterized by S-S symmetric bending (δ) and stretching (ν) modes at 240 ± 5 and 538 ± 5 cm^{-1}, respectively, and corresponding overtones $\delta_s + \nu_s$, $2\nu_s$, $3\nu_s$, and $4\nu_s$, due to the Raman resonance phenomenon of S_3^- at the wavelength of the He-Ne laser (*14*–*19*). Kinetic and heating-cooling measurements (*13*) show that this species forms rapidly and reversibly at the expense of sulfate and sulfide (figs. S4 and S5). Owing to the radical nature of S_3^- that allows fast electron transfer, its presence accelerates the attainment of the sulfide-sulfate equilibrium at moderate temperatures (250° to 300°C) and near-neutral pH (6 to 8). Our findings demonstrate that S_3^- is a dominant, thermodynamically stable aqueous sulfur form at least in the range 250° to 450°C and 0.5 to 3.5 GPa.

The fast breakdown of S_3^- to sulfate and sulfide (with or without native sulfur) below 250°C explains the absence of reports of S_3^- in numerous studies employing fluid sampling or quenching techniques (*4*, *9*, *11*). The few in situ studies conducted so far using ultraviolet-visible (*20*) and Raman spectroscopy (*21*) in sulfur-bearing aqueous solutions at similar temperatures (150° to 500°C), but at much lower pressures (<0.1 GPa), may have erroneously attributed the S_3^- spectral pattern to other species. Compared with those

data, our high-pressure results indicate a larger S_3^- stability domain in temperature, acidity, and sulfur concentration. This pressure-driven stabilization in dense aqueous solution may be due to solvation of S_3^- by water molecules yielding energetically favorable coordination geometries, similar to those in zeolite cages of ultramarine-type minerals in which tetrahedral coordination of S_3^- by Na^+ strongly stabilizes this radical ion (*18*). The structure of S_3^- with an S–S–S angle of 103° (*17*), close to that of H–O–H in H_2O, may favor its incorporation into the tetrahedral network of hydrogen bonds formed by water molecules in the dense liquid phase at elevated pressure.

We estimated the S_3^- concentrations from comparison of the Raman intensities of the nonresonant sulfate and sulfide species and using the mass balance of the total dissolved sulfur and constraints of the relative fractions of S^{6+} and S^{2-} forms imposed by the system composition (*13*). These data, combined with the robust thermodynamic properties for sulfate and sulfide species (*8*, *12*), allow derivation of S_3^- formation constants (*22*) and prediction of S_3^- equilibrium amounts in natural fluids (Fig. 3). In an aqueous solution at 350°C and 0.5 to 1.5 GPa with 1 wt % S, which is a common S concentration for Au-Cu–bearing fluids in porphyry systems (*3*, *23*) and metamorphic fluids generated by pyrite breakdown (*24*), S_3^- accounts for a major part of dissolved sulfur (>50 to 95%) in a wide range of pH (2 to 7) at oxygen fugacity of the hematite-magnetite (HM) buffer. In more reducing environments, like those of the mantle-crust boundary or serpentinization processes in subduction zones, approximated by the nickel-nickel oxide or quartz-fayalite-magnetite (QFM) equilibria, the S_3^- ion attains amounts comparable with H_2S in fluids with ≥1000 parts per million (ppm) of dissolved S at near-neutral pH.

The S_3^- ion has been studied extensively at low-pressure conditions in nonaqueous chemical systems such as sulfur-bearing organic solvents, alkali halide polysulfide solids and melts, S-doped aluminoborosilicate glasses, ultramarine pigments, and zeolite minerals such as lapis lazuli (*14*–*19*). However, the formation of S_3^- also has consequences for sulfur geochemistry and metal transport in high-temperature and -pressure crustal and mantle fluids. First, the formation of S_3^- at the expense of H_2S/HS^- and SO_4^{2-} (Fig. 3) will enhance the sulfur mobility in the fluid phase by reducing the amount of sulfur retained in pyrite, pyrrhotite, anhydrite, and barite, the major sulfur-bearing minerals. In metamorphic settings of greenschist-amphibolite facies, S_3^- will widen the temperature-pressure window of pyrite breakdown leading to generation of sulfur-rich fluids (*24*). In subduction processes, a part of oceanic crust sulfur is transported along the slab down to zones of dehydration and partial melting (*3*, *25*, *26*). If S_3^- also forms at magmatic temperatures, as indicated by analyses of synthetic silicate glasses (*19*), it will enhance the release of sulfur from the FeS-bearing silicate melt into the degassing aqueous fluid phase, contributing to the sulfur flux in volcanic arcs. Evolved arc magmas and associated fluids are often characterized by high oxygen fugacity, up to QFM+2 (*3*, *26*), favoring S_3^- stability.

Second, because of its similarity to polysulfide ions like S_3^{2-} and S_2^{2-} that form strong complexes with Au in aqueous solution (*27*), S_3^- should exhibit a high affinity for Au and similar metals (Cu, Pt). This ligand will thus efficiently compete with HS^- and H_2S, which are regarded so far as the main transporting agents of gold in hydrothermal fluids (*2*, *12*, *23*, *24*). Experimental evidence (*12*, *28*) in S-rich solutions at 300° to 600°C and 0.05 to 0.5 GPa of Au solubilities up to three orders of magnitude higher than can be explained by the known Au(I)-sulfide complexes $AuHS^0$ and $Au(HS)_2^-$ (*2*, *11*, *12*) may be due to Au binding with S_3^-. Optimal conditions for S_3^- formation include temperatures around 350°C, redox conditions close to the HM buffer, and dissolved S concentrations above 1000 ppm (Fig. 3). Such conditions are met in porphyry and epithermal Au-Cu deposits associated with active convergent margins on Earth (*3*, *23*). Aqueous S_3^- released at high pressures from arc magmas into the fluid phase in such settings may extract Au and Cu from the slab and/or mantle wedge. Upon the fluid ascent and pressure decrease, S_3^- will decompose into sulfate and sulfide. This may result in partial gold precipitation via sulfidation reactions with Fe-bearing rocks in porphyry and orogenic deposits (*3*, *25*, *29*), whereas some part of Au and associated metals (Cu, Se, Te) may be transported upward to shallow epithermal deposits by the low-density vapor phase as volatile species with H_2S and/or SO_2 (*11*, *23*). Thus, S_3^- may not only enhance the mobility of chalcophile metals at depth, but it may also provide the source of sulfur and metals for the important types of gold deposits in Achaean greenstone belts and porphyry-epithermal systems that imply high gold and sulfur fluxes over a wide temperature-pressure-acidity range (*3*, *23*, *29*) favored by the elevated solubility of S_3^-.

Third, if S_3^- is abundant in hydrothermal fluids, it will influence thermodynamic properties of intermediate-valence aqueous sulfur species (*8*, *11*, *12*, *20*, *24*) and kinetic models of reactions between sulfates and sulfides (*4*, *30*) in aqueous solution at high temperatures and pressures. This may, in turn, affect sulfur isotope–fractionation models (*4*–*7*, *25*, *30*), which ignore the formation of S_3^- in geological fluids.

References and Notes

1. C. W. Mandeville, *Elements* **6**, 75 (2010).
2. H. L. Barnes, Ed., *Geochemistry of Hydrothermal Ore Deposits* (Wiley, New York, 1997).
3. J. W. Hedenquist, J. B. Lowenstern, *Nature* **370**, 519 (1994).
4. H. Ohmoto, A. C. Lasaga, *Geochim. Cosmochim. Acta* **46**, 1727 (1982).
5. H. Ohmoto, Y. Watanabe, H. Ikemi, S. R. Poulson, B. E. Taylor, *Nature* **442**, 908 (2006).
6. J. Farquhar *et al.*, *Nature* **449**, 706 (2007).
7. P. Philippot *et al.*, *Science* **317**, 1534 (2007).
8. J. W. Johnson, E. H. Oelkers, H. C. Helgeson, *Comput. Geosci.* **18**, 899 (1992) and references therein.
9. T. P. Dadze, V. I. Sorokin, *Geochem. Int.* **30**, 38 (1993).
10. M. Kusakabe, Y. Komoda, B. Takano, T. Abiko, *J. Volcanol. Geotherm. Res.* **97**, 287 (2000).
11. G. S. Pokrovski, A. Y. Borisova, J.-C. Harrichoury, *Earth Planet. Sci. Lett.* **266**, 345 (2008).
12. G. S. Pokrovski, B. R. Tagirov, J. Schott, J.-L. Hazemann, O. Proux, *Geochim. Cosmochim. Acta* **73**, 5406 (2009).
13. Materials and methods and other supporting material are available on *Science* Online.
14. T. Chivers, *Nature* **252**, 32 (1974).
15. T. Chivers, I. Drummond, *Inorg. Chem.* **11**, 2525 (1972).
16. T. Chivers, C. Lau, *Inorg. Chem.* **21**, 453 (1982).
17. R. J. H. Clark, D. G. Cobbold, *Inorg. Chem.* **17**, 3169 (1978).
18. D. Reinen, G.-G. Lindner, *Chem. Soc. Rev.* **28**, 75 (1999).
19. K. B. Winther, E. B. Watson, G. M. Korenowski, *Am. Mineral.* **83**, 1141 (1998).
20. W. Giggenbach, *Inorg. Chem.* **10**, 1306 (1971).
21. G. V. Bondarenko, Y. E. Gorbaty, *Geochim. Cosmochim. Acta* **61**, 1413 (1997).
22. Obtained values correspond to the following decimal logarithms of the thermodynamic equilibrium constant of the reaction: $2\ H_2S(aq) + SO_4^{2-} + H^+ = S_3^- + 0.75\ O_2(gas) + 2.5\ H_2O$; $\log_{10}K = -16.2 \pm 1.8$, -9.6 ± 1.7, -11.7 ± 3.1, and -9.2 ± 2.9 at 300°, 350°, 400°, and 450°C, respectively. These values are independent of pressure within errors from 0.5 to 1.5 GPa. The uncertainties (±1 SD) mainly stem from (i) determination of species amounts from Raman spectra and (ii) extrapolation of thermodynamic properties of aqueous species above 0.5 GPa (*13*). The values indicate that the stability of S_3^- increases greatly from 300° to 350°C and remains constant within errors to at least 450°C.
23. J. H. Seo, M. Guillong, C. A. Heinrich, *Earth Planet. Sci. Lett.* **282**, 323 (2009).
24. A. G. Tomkins, *Geochim. Cosmochim. Acta* **74**, 3246 (2010).
25. J. C. M. de Hoog, P. R. D. Mason, M. J. van Bergen, *Geochim. Cosmochim. Acta* **65**, 3147 (2001).
26. K. A. Kelley, E. Cottrell, *Science* **325**, 605 (2009).
27. M. E. Berndt, T. Buttram, D. Earley III, W. E. Seyfried Jr., *Geochim. Cosmochim. Acta* **58**, 587 (1994).
28. R. R. Loucks, J. A. Mavrogenes, *Science* **284**, 2159 (1999).
29. E. J. Mikucki, *Ore Geol. Rev.* **13**, 307 (1998).
30. X. Chu, H. Ohmoto, D. R. Cole, *Chem. Geol.* **211**, 217 (2004).

31. This work was supported by Institut National des Sciences de l'Univers–CNRS grants 3F, SOUMET, and CO2MET; a transnational access grant to the European High-Pressure Facility of Bayerisches Geoinstitut; and a Deutscher Akademischer Austausch Dienst–Partenariat Hubert Curien linkage grant PROCOPE. We thank L. Kison-Herzing, S. Linhardt, S. Übelhack, D. Krauße, and C. Cavaré-Hester for technical and logistical support and J. Schott, A. Borisova, N. Dubrovinskaia, Y. Shvarov, and H. Keppler for advice. The article benefited from comments of three anonymous reviewers.

Supporting Online Material

www.sciencemag.org/cgi/content/full/331/6020/1052/DC1
Materials and Methods
SOM Text
Figs. S1 to S5
Tables S1 and S2
References

2 November 2010; accepted 4 January 2011
10.1126/science.1199911